Available online at www.sciencedirect.com
ScienceDirect
International Journal of Heat and Mass Transfer 51 (2008) 3963–3971
International Journal of HEAT and MASS TRANSFER
www.elsevier.com/locate/ijhmt

Effect of corrugated plates in an in-phase arrangement on the heat transfer and flow developments

Paisarn Naphon *

Thermo-Fluid and Heat Transfer Enhancement Laboratory (TFHT), Department of Mechanical Engineering, Faculty of Engineering, Srinakharinwirot University, 63 Rangsit-Nakhornnayok Road, Ongkharak, Nakhorn-Nayok 26120, Thailand

Received 21 May 2007; received in revised form 30 November 2007
Available online 7 March 2008

Abstract

In the present study, the numerical results of the heat transfer and flow developments in the corrugated channel under constant heat flux conditions are presented. The test section is the channel with two opposite corrugated plates which all configuration peaks lie in an in-phase arrangement. The corrugated plates with three different corrugated tile angles of 20°, 40°, and 60° are tested with the height of the channel of 12.5 mm. The model was simulated for the Reynolds number and heat flux in the ranges of 400–1600 and 0.5–1.2 kW/m^2, respectively. The flow and heat transfer developments are simulated by using the k-ε standard turbulent model. A finite volume method with the structured uniform grid system is employed for solving the model. The predicted results are validated by comparing with the measured data. There is reasonable agreement from the comparison between the numerical data and experimental data. Effects of relevant parameters on the heat transfer and flow developments are discussed. Due to the breaking and destabilizing in the thermal boundary zone, the corrugated surface has significant effect on the enhancement of heat transfer and pressure drop.

Keywords: Heat transfer development; Flow development; Corrugated channel

1. Introduction

As fluid flowing through the corrugated surfaces, the breaking and destabilizing in the thermal boundary zone are induced. The heat transfer rate (thermal performance) of the heat transfer devices tends to increase. Therefore, the corrugated surfaces are a suitable method to improve the thermal performance of heat transfer devices. Sunden et al. [1,2] experimentally and numerically studied on the heat transfer and pressure drop in the corrugated channels and the smooth tubes under constant heat flux conditions. It was found that the heat transfer obtained from the corrugated channel was 3.5 times higher than that from the smooth one. Brunner and Brenig [3] calculated the scattering of molecules from the corrugated surfaces with rotational energy transfer. Benilov and Yaremchuk [4] investigated the scattering of surface water-waves in a channel with corrugated bottom and walls. Yalamanchili et al. [5,6] applied the LDV to measure the velocity profiles and normal stress of fluids flowing in a corrugated channel with the top and bottom plates sinusoidal with and without polymer additives. Sawyers et al. [7] numerically and experimentally studied effect of three dimensional hydrodynamics on the enhancement of heat transfer in the corrugated channels. Nishimura and Matsune [8] studied on the simulation and flow visualization to study the dynamical behavior of vortices generated in channels with two different geometries. Bereiziat and Devienne [9] experimentally studied the flow characteristics of the Newtonian and non-Newtonian fluid in the corrugated channel. Gradeck et al. [10,11] observed flow patterns and heat transfer analysis of single phase and two phase gas-liquid flowing in the horizontal corrugated channels. Fabbri et al. [12,13] studied the laminar convective heat transfer in the smooth and corrugated channels. The heat transfer performance

* Tel.: +663 7322625x2065; fax: +663 7322609.
E-mail address: paisarnn@swu.ac.th

0017-9310/$ - see front matter © 2008 Elsevier Ltd. All rights reserved.
doi:10.1016/j.ijheatmasstransfer.2007.11.050

Nomenclature

A	area
$C_{\varepsilon 2}$	turbulent model constant
C_p	specific heat, kJ/(kg °C)
h	heat transfer coefficient, kW/(m^2 °C)
I	turbulent intensity
L	turbulence characteristics length, m
Nu	Nusselt number
Pr	Prandtl number
Q	heat transfer rate, kW
Re	Reynolds number
U	velocity vector
ρ	density, kg/m^3
Φ	viscosity energy dissipation function
σ_ε	diffusion Prandtl number for ε
$\overline{X}$	distance from the leading edge of the corrugated plate
$\overline{\sigma}$	distance the leading edge of the corrugated along the corrugated surface, m
κ	thermal conductivity, kW/(m °C)
$C_{\varepsilon 1}$	turbulent model constant
C_μ	turbulent model constant
D_h	hydraulic diameter, m
H	height of channel, m
k	turbulent kinetic energy, m^2/s^2
m	mass flow rate, kg/s
p	pressure, kPa
P	wet perimeter, m
q	heat flux, kW/m^2
T	temperature, °C
ε	dissipation kinetic energy, m^2/s^3
μ	viscosity, kg/m
σ_k	diffusion Prandtl number for k
τ	shear stress, kN/m^2

Subscripts

a	air
cr	cross section
in	inlet
ave	average
c	corrugated
out	outlet

of the corrugated channel was compared with that of a smooth channel. Mehrabian and Poulter [14] studied effect of corrugation angle on the performance of the flowing between two identical APV SR3 plates. Vasudevaiah and Balamurugan [15] theoretically studied the convective heat transfer in a corrugated microchannel under constant heat flux conditions. Niceno and Nobile [16] numerical studied on the two-dimensional steady state and time dependent fluid flow and heat transfer in the periodic and wavy channels. Hamza et al. [17] experimentally studied effects of the operating parameters on laminar flow forced-convection heat transfer of air flowing in a channel having a V-corrugated upper plate. Zimmerer et al. [18] studied effects of the inclination angle, the wavelength, the amplitude, and the shape of the corrugation on the heat and mass transfer of the heat exchanger. Wang and Chen [19] applied a simple coordinate transformation method and the spline alternating-direction implicit method for determining the heat transfer rates for flowing through a sinusoidally curved converging–diverging channel. Metwally and Manglik [20] considered the laminar periodically developed forced convection in sinusoidal corrugated-plate channels. The control volume finite-difference method was employed to solve the model. Islamoglu and Parmaksizoglu [21–23] numerically and experimentally studied effect of channel height on the enhanced heat transfer characteristics in a corrugated heat exchanger channel. In addition, the artificial neural networks were employed to analyze the heat transfer in corrugated channels Hossain and Sadrul Islam [24] numerical studied on the fully unsteady fluid flow and heat transfer in sine shaped wavy channels. Recently, Naphon [25,26] experimentally studied on the heat transfer characteristics and pressure drop in the corrugated channel with different wavy angles and channel heights. The corrugated plates in an in-phase and out-of-phase arrangements were tested.

The above survey, the numerous experimental and theoretical studies have been reported concerning the heat transfer and pressure drop in the corrugated surface with various configurations. However, only a few works [17,21–23] reported on heat transfer characteristics and pressure drop in the corrugated channel with V-corrugated upper and lower plates. The objective of this paper is to numerical and experimental study the heat transfer and flow developments in the channel with V-corrugated upper and lower plates which all configuration peaks lie in an in-phase arrangement. The predicted results are validated by comparing with the measured data. The temperature and velocity distributions are simulated by the finite volume method. Effects of various relevant parameters on the heat transfer and flow developments are also considered.

2. Experimental apparatus and method

2.1. Test loop

A schematic diagram of the experimental apparatus is shown in Fig. 1. The test section and the connections of the piping system are designed such that parts can be changed or repaired easily. The open-loop wind tunnel is rectangular air duct fabricated from acrylic having the length of 295 cm. The duct is insulated with 5 mm thick Aeroflex

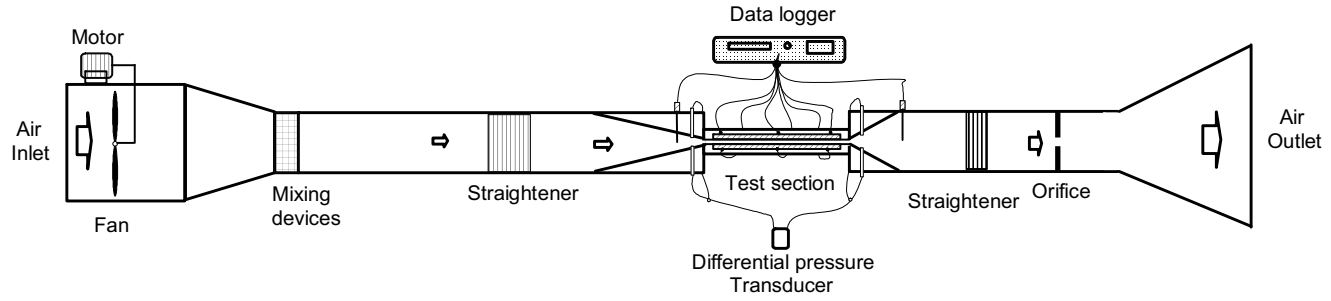

Fig. 1. Schematic diagram of experimental apparatus.

standard sheet. Air in the open wind tunnel is discharged by an axial fan into the channel and is passed through a mixing device, straightener, test section, orifice and then discharged to the atmosphere. The speed of the axial fan can be adjusted by a variable speed driver. An orifice plate based on the ISO 5167 standard is employed to measure air flow rate. The pressure drops across the test section and orifice plate are measured by the digital manometer (TESTO 400) with an accuracy of 0.02% of full scale. There are four pressure taps on each wall upstream and downstream of the test section and the orifice plate. The inlet and outlet temperatures of air are measured by two and four type *T* copper–constantan thermocouples with 1 mm diameter probes with an accuracy of 0.1% of full scale extending into the duct in which the air flows, respectively. All the thermocouples probes are precalibrated by dry-box temperature calibrator with 0.01 °C precision.

2.2. Test sections

The schematic diagram of the test section is shown in Figs. 2 and 3 which consists of two opposite corrugated plates. The width and length of the corrugated plate are 130 and 300 mm, respectively. The details of the corrugated plate are listed in Table 1. An AC power supply is the source of power for the plate type heaters, used for heating of the test section. Both rear faces of the test section are insulated with a 10 mm thick heat-resistant mica standard sheet, 5 mm thick aeroflex standard sheet, and then 5 mm thick acrylic standard sheet, respectively. Three type *T* copper–constantan thermocouples are used to measure the temperature distribution of each corrugated wall. The thermocouples were installed by drilling from the rear face and fixed with special glue applied to the rear face of the corrugated walls.

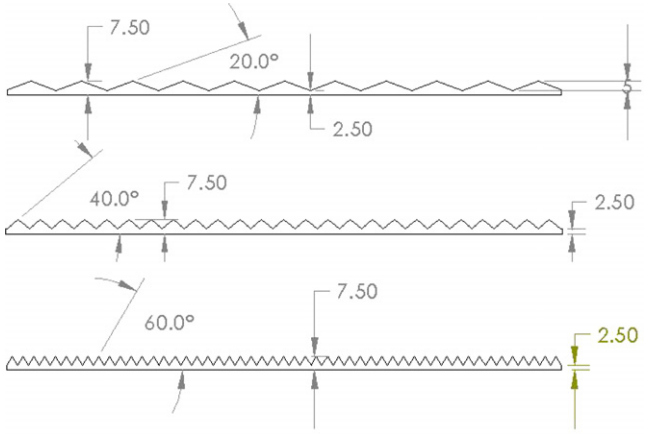

Fig. 3. Schematic diagram of the corrugated plate.

2.3. Operating conditions

Experiments were done with various air flow rates and heat flux entering the test section. In the experiments, air flow rate was increased in small increments while the supplied heat at both sides of the corrugated wall was kept constant. The supplied heat into the corrugated walls was adjusted to achieve the desired level by using electric heaters. The voltage and current of electric input to the cartridge heaters were controlled by an AC power supply unit. The supplied power was calculated using the supplied

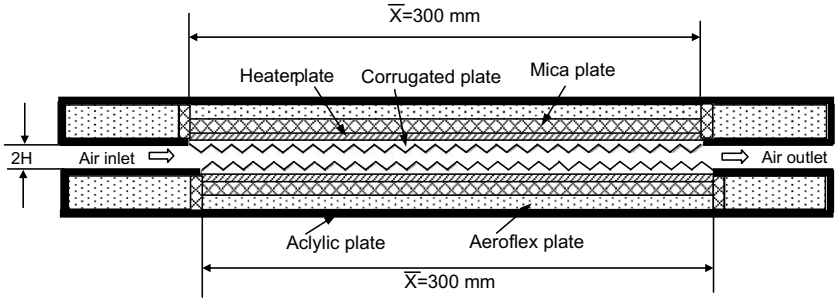

Fig. 2. Schematic diagram of the test section.

Table 1
Dimensions of the test section

Wavy angle (°)	Height of channel (mm)	Height of wavy (mm)	Height of base (mm)	Width of corrugated channel (mm)	Length of corrugated channel (mm)	Number of wavy	Length of corrugated surface (mm)	Total surface area (m^2)
20	12.5	5	2.5	130	300	11	320	0.043
40	12.5	5	2.5	130	300	25	389	0.052
60	12.5	5	2.5	130	300	52	600	0.073

Table 2
Accuracy and uncertainty of measurements

Instruments	Accuracy	Uncertainty
Thermocouple type *T*, data logger, (°C)	0.1%	±0.1
Differential pressure transducer	0.02%	±0.02

voltage and current to the heaters. The supplied voltage and current to the heaters were measured by the digital clamp meter (3PK-2002 A). The steady-state sensible heat gain by the air flow can be calculated from an energy balance. In the present study, only the data that satisfy the energy balance conditions; $|Q_{heater} - Q_a|/Q_{ave}$ is less than 10%, are used in the analysis. The average heat transfer, Q_{ave}, is averaged from the supplied heat to the heater and the removed heat by cooling air. The temperature at each position and pressure drop across the test section were recorded three times. Data collection was carried out using a data acquisition system (DataTaker, DT800). Temperatures at each position and pressure drops across the test section were averaged over the time period. The uncertainty and accuracy of the measurement are given in Table 2.

The average heat transfer coefficient along the corrugated channel, h_c, can be calculated from the average heat transfer rate obtained from

$$Q_{ave} = h_c A_c (\Delta T) \tag{1}$$

where A_c is the surface area of the corrugated plate.

In general, an average heat transfer coefficient is presented in term of average Nusselt number (see Wang and Chen [19]) as follows:

$$Nu = \frac{h_c H \bar{\sigma}}{\kappa \overline{X}} \tag{2}$$

where H is the half distance of the channel height, κ is the thermal conductivity of air, $\overline{X}$ is the distance from the leading edge of the corrugated plate, and $\overline{\sigma}$ is the distance the leading edge of the corrugated along the corrugated surface.

3. Mathematical modelling

By considering the geometry and physical problem as shown in Figs. 2 and 4, the k–ε standard turbulence model [27,29] is employed to simulate the turbulent heat transfer and flow characteristics. The main governing equations [27,29] can be written in the following form:

Continuity equation:

$$\frac{\partial \rho}{\partial t} + \mathrm{div}(\rho U) = 0 \tag{3}$$

Momentum equation:

$$x - \mathrm{momentum} : \rho \frac{\mathrm{D}u}{\mathrm{D}t} = -\frac{\partial p}{\partial x} + \mathrm{div}(\mu\ \mathrm{grad}\ u) + S_{M_x} \tag{4}$$

$$y - \mathrm{momentum} : \rho \frac{Dv}{Dt} = -\frac{\partial p}{\partial y} + \mathrm{div}(\mu\ \mathrm{grad}\ v) + S_{M_y} \tag{5}$$

Energy equation:

$$\rho \frac{\mathrm{D}i}{\mathrm{D}t} = -p\mathrm{div}U + \mathrm{div}(\Gamma\ \mathrm{grad}\ T) + \Phi + S_i \tag{6}$$

Turbulent kinetic energy (k) equation:

$$\frac{\partial(\rho k)}{\partial t} + \mathrm{div}(\rho k U) = \mathrm{div}\left[\left(\frac{\mu_t}{\sigma_k}\mathrm{grad}\ k\right)\right] + 2\mu_t E_{ij} \cdot E_{ij} - \rho\varepsilon \tag{7}$$

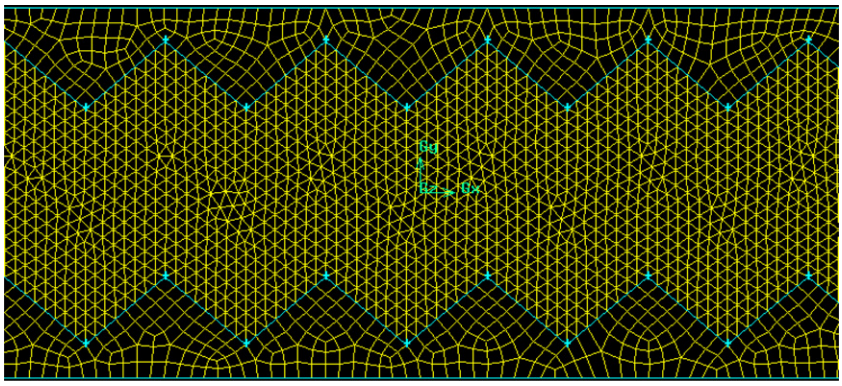

Fig. 4. Schematic diagram of the structured uniform grid systems.

Turbulent kinetic energy dissipation (ε) equation:

$$\frac{\partial(\rho\varepsilon)}{\partial t} + \mathrm{div}(\rho\varepsilon U) = \mathrm{div}\left(\frac{\mu_t}{\sigma_\varepsilon}\ \mathrm{grad}\ \varepsilon\right) + C_{1\varepsilon}\frac{\varepsilon}{k}2\mu_t E_{ij}\cdot E_{ij} - C_{2\varepsilon}\rho\frac{\varepsilon^2}{k} \quad (8)$$

The empirical constants for the turbulence model are arrived by comprehensive data fitting for a wide range of turbulent flow of Launder and Spalding [28,29]:

$$C_\mu = 0.09, C_{\varepsilon 1} = 1.47, C_{\varepsilon 2} = 1.92, \sigma_k = 1.0, \sigma_\varepsilon = 1.3 \quad (9)$$

Boundary conditions:

In the present study, noslip and constant heat flux boundary conditions are applied on the test section as follows:

$$u = 0, v = 0, q = q_{wall} \quad (10)$$

where u, v are the velocities.

Initial conditions:

At the inlet boundary condition, the uniform profiles for all the properties are as follows:

$$u = u_{in}, v = 0, T = T_{in}, k = k_{in}, \varepsilon = \varepsilon_{in} \quad (11)$$

The turbulent kinetic energy, k_{in}, and the turbulent kinetic energy dissipation, ε_{in}, at the inlet section are approximated from the turbulent intensity, I, and a turbulent characteristics length, L, as follows:

$$k_{in} = \frac{3}{2}(u_{in}I)^2, \varepsilon_{in} = C_\mu^{3/4}\frac{k^{3/2}}{L} \quad (12)$$

In the present study, the turbulence characteristics length, L, is set to be $0.07r_h$. The factor of 0.07 is based on the maximum value of the mixing length in the fully developed turbulent flow [29]. The turbulent intensity level, I, is defined the ratio of the root-mean-square of the velocity fluctuation, u', to the mean flow velocity, u, as follows:

$$I = \frac{u'}{u}\times 100\% \quad (13)$$

To represent the results and characterize the heat transfer and flow in the corrugated channel, the following variables and parameters are presented:

$$T_{a,b} = \frac{\int_0^{A_{cr}} uT_a dA_{cr}}{\int_0^{A_{cr}} u dA_{cr}} \quad (14)$$

$$Nu = \frac{(Q_{ave}/A_c)\cdot d_h}{\kappa(T_{s,ave} - T_{a,b})}, T_{s,ave} = \frac{1}{\overline{\sigma}}\int_0^{\overline{\sigma}} T_{s,x}dx \quad (15)$$

where u is the axial velocity, $T_{s,x}$, $T_{s,ave}$ are the local and average surface temperatures, respectively, $T_{a,b}$ is the bulk temperature of air, d_h and r_h are the hydraulic diameter and hydraulic radius, respectively.

4. Numerical computation

The governing equations (3)–(13) are a set of convection equations with velocity and pressure coupling. Based on the control volume method, SIMPLEC algorithm of Van Doormal and Raithby [30] is employed to deal with the problem of velocity and pressure coupling. Second-order upwind scheme and structured uniform grid system are used to discretize the main governing equations as shown in Fig. 4. In order to obtain the satisfactory solutions, the grid independence is carried out in the analysis by adopting different grid distributions of 60,000, 120,000, and 210,000. The grid independence test indicated that the grid systems of 120,000 ensure a satisfactory solution. This is verified by the fact that the difference of the computed results of outlet air temperature, corrugated plate temperature and the Nusselt number with grid finer than the 120,000 (e.g. 210,000) within 1%. At the inlet, fluid with turbulence intensity, I, and temperature, T_{in}, enters the test section at the velocity of u_{in}. Velocity boundary condition is applied at the inlet section while the pressure boundary condition is used at the outlet section. The commercial program NASTRAN/CFDsign has been employed as the numerical solver. The numerical computation is ended if the residual summed over all the computational nodes satisfies the criterion (10^{-5}).

5. Results and discussion

Because there is almost no data as in the open literature [1–23] on the heat transfer and flow characteristics in the V-corrugated channel, the predicted results are compared with the present experimental data as shown in Figs. 5–7. Fig. 5 shows the comparison between the predicted outlet air temperature and the measured ones. It can be clearly seen from figure that the values obtained from the model are consistent with the experimental data and lie within ±10%. Figs. 6 and 7 show the comparison between the predicted plate temperature, the predicted Nusselt number and

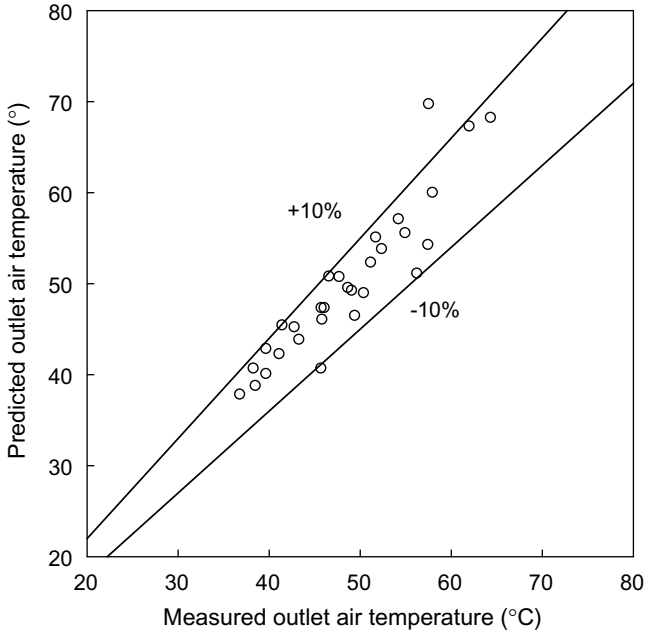

Fig. 5. Comparison of the measured data with the predicted result.

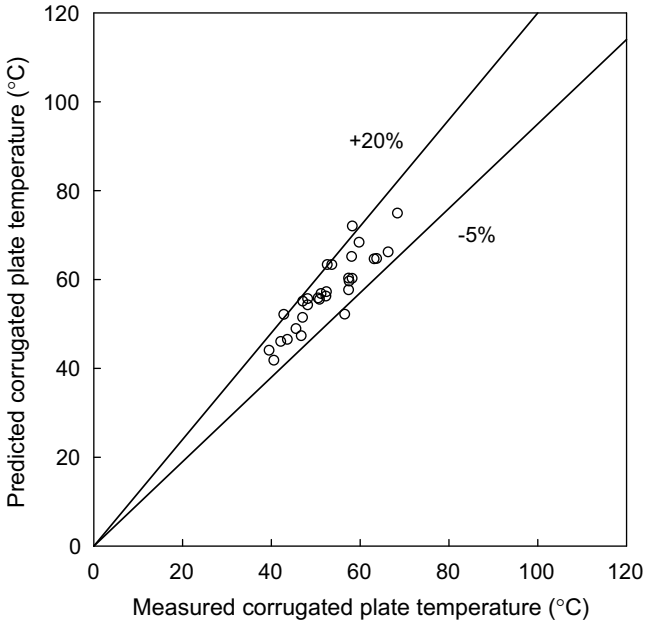

Fig. 6. Comparison of the measured data with the predicted result.

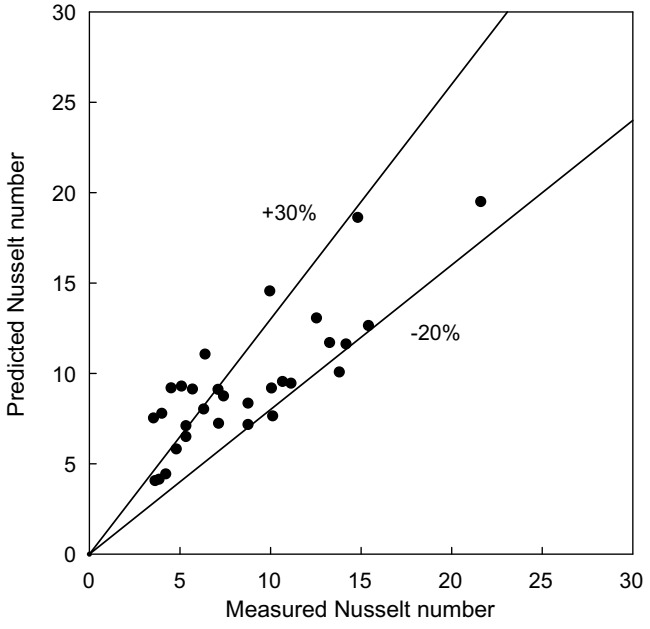

Fig. 7. Comparison of the measured data with the predicted result.

the measured data, respectively. The average plate temperature and average Nusselt number are calculated from Eq. [15]. It can be noted that the values obtained from the model are consistent with the experimental data and lie within −5% to +20% for the average plate temperature and −20% to +30% for the average Nusselt number.

Fig. 8 shows the variation of the average plate temperature with air Reynolds number for different wavy angles at heat flux of 1.08 kW/m^2. It can be seen that the heat transfer rate depends on the cooling capacity rate of air. Therefore, the average plate temperature decreases as air

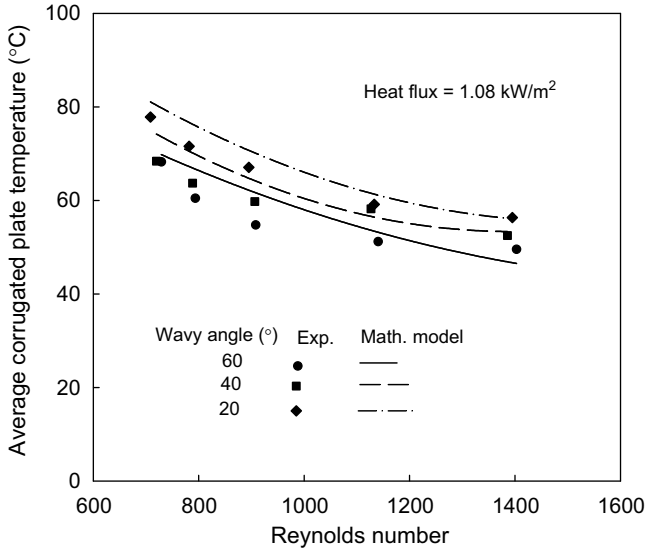

Fig. 8. Variation of average surface plate temperature with Reynolds number for different wavy angle.

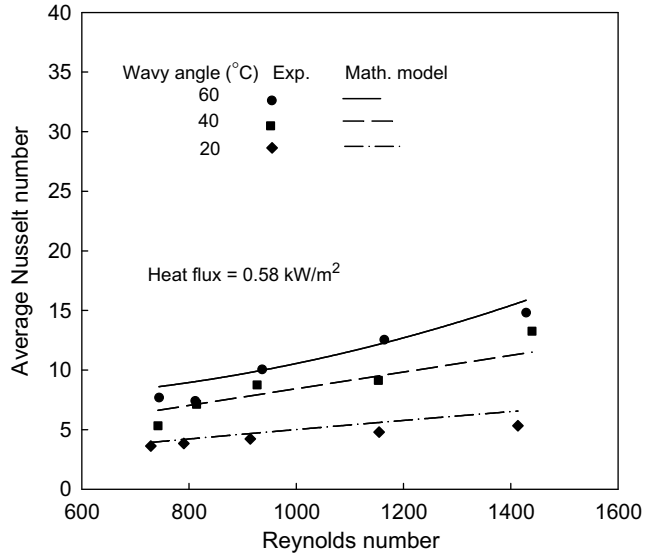

Fig. 9. Variation of Nusselt with Reynolds number for different wavy angle.

Reynolds number increases. However, this effect tends to diminish as Reynolds number further increases. In addition, for a given air flow rate, average plate temperatures at higher wavy angle are lower than those from lower ones. Due to higher surface area and higher fluid mixing in the boundary layer zone, heat transfer from the surface to the air also increases. Therefore, the higher wavy angles give lower plate temperatures as shown in Fig. 8. The predicted results are compared with the measured data. In general, the shape of the predicted and observed average corrugated plate temperature profiles agree well.

Fig. 9 shows the variation of average Nusselt number with air Reynolds number. It can be seen that with increas-

ing air Reynolds number, the Nusselt number tends to increase. In generally, as fluid flowing through the corrugated surface the fluid re-circulation or/and the swirl flows are generated in the corrugation troughs. The onset and growth of recirculation zones promote the mixing of fluid in the boundary layer thereby enhancing the convective heat transfer. Fig. 9 also shows effect of wavy angle on the Nusselt number. It can be clearly seen from figure that the Nusselt numbers at higher wavy angle are higher than those at lower ones. Increase wavy angle, higher of fluid re-circulation or/and higher swirl flows intensity in the corrugation troughs, and larger surface area, therefore the Nusselt number also increases with increasing wavy angle.

Fig. 10 shows the temperature contour and velocity vector for different wavy angle at $q = 1.08$ kW/m^2, $Re = 1395$. It is clearly seen from the Fig. 10a that the onset and the growth of the swirl flow promote the mixing of the cold fluid from the core with the hot fluid near the boundary layer. These results induce higher temperature gradient near the wavy wall. Therefore, the net heat transfer rate from the wavy wall to the fluid also enhances as wavy angle increases. Fig. 10b also shows the variation of the velocity

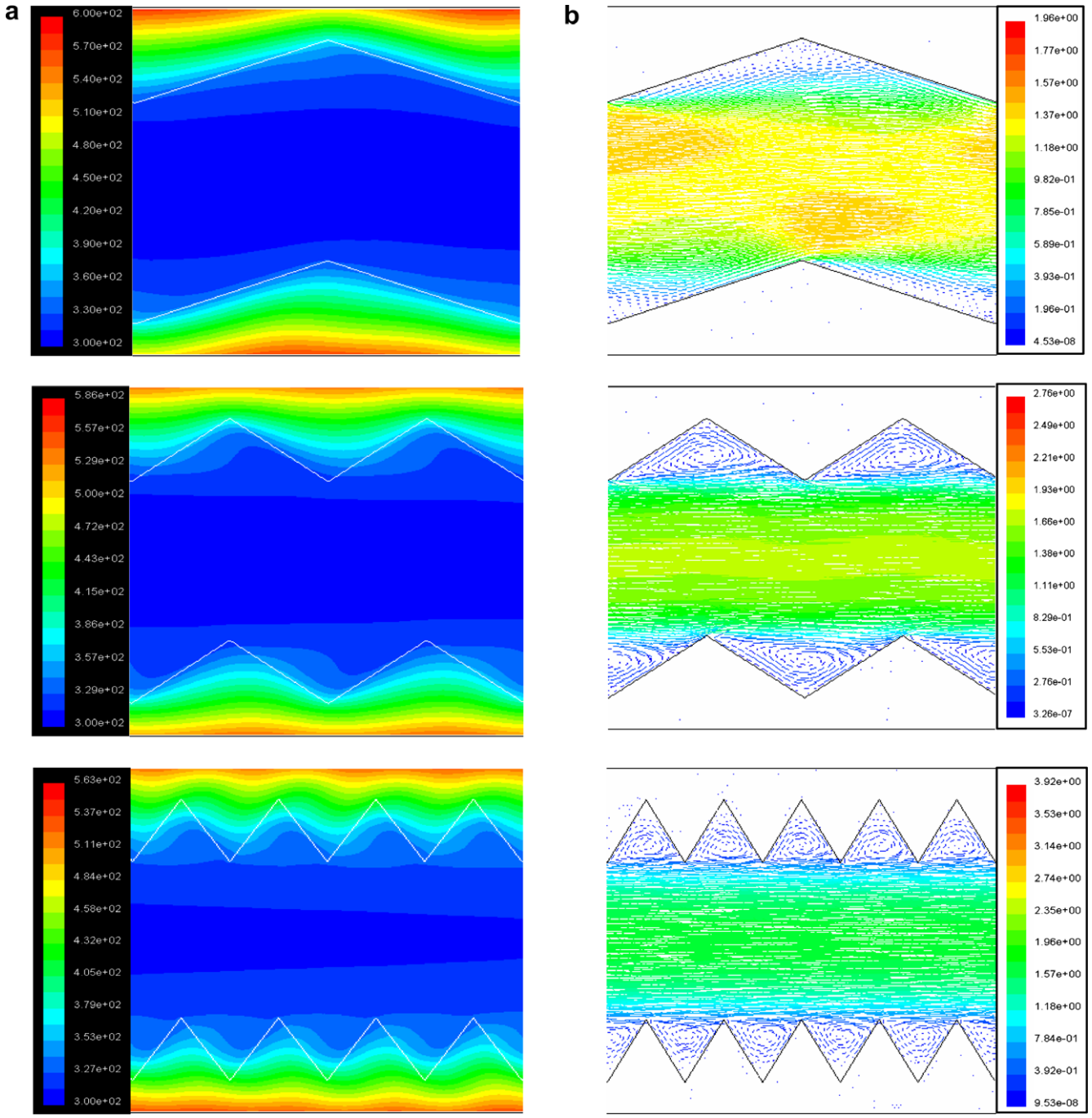

Fig. 10. Variation of (a) temperature contour, (b) velocity vector for different wavy angles (20°, 40°, 60°) at $q = 1.08$ kW/m^2, $Re = 1395$, $2H = 12.5$ mm.

vector for different wavy angle at $Re = 1395$, $2H = 12.5$ mm. It is can be seen that the wavy geometry has insignificant effect on the core flow. In addition, at low wavy angle, the wavy geometry has slightly effect on the flow, and the fluid moves undisturbed through the channel with no re-circulation. However, as further increasing wavy angle (decreasing pitch), fluid re-circulation or swirl flows are induced in the corrugated troughs, and consequently higher momentum transfer.

Fig. 11 shows the temperature contour and velocity vector for different channel heights (12.5, 7.5, 5.0 mm) for wavy angle of 40°, constant heat flux of 0.83 kW/m^2, and constant air flow rate ($Re = 9138$). It is can be seen that the wavy wall has a significant effect on the temperature

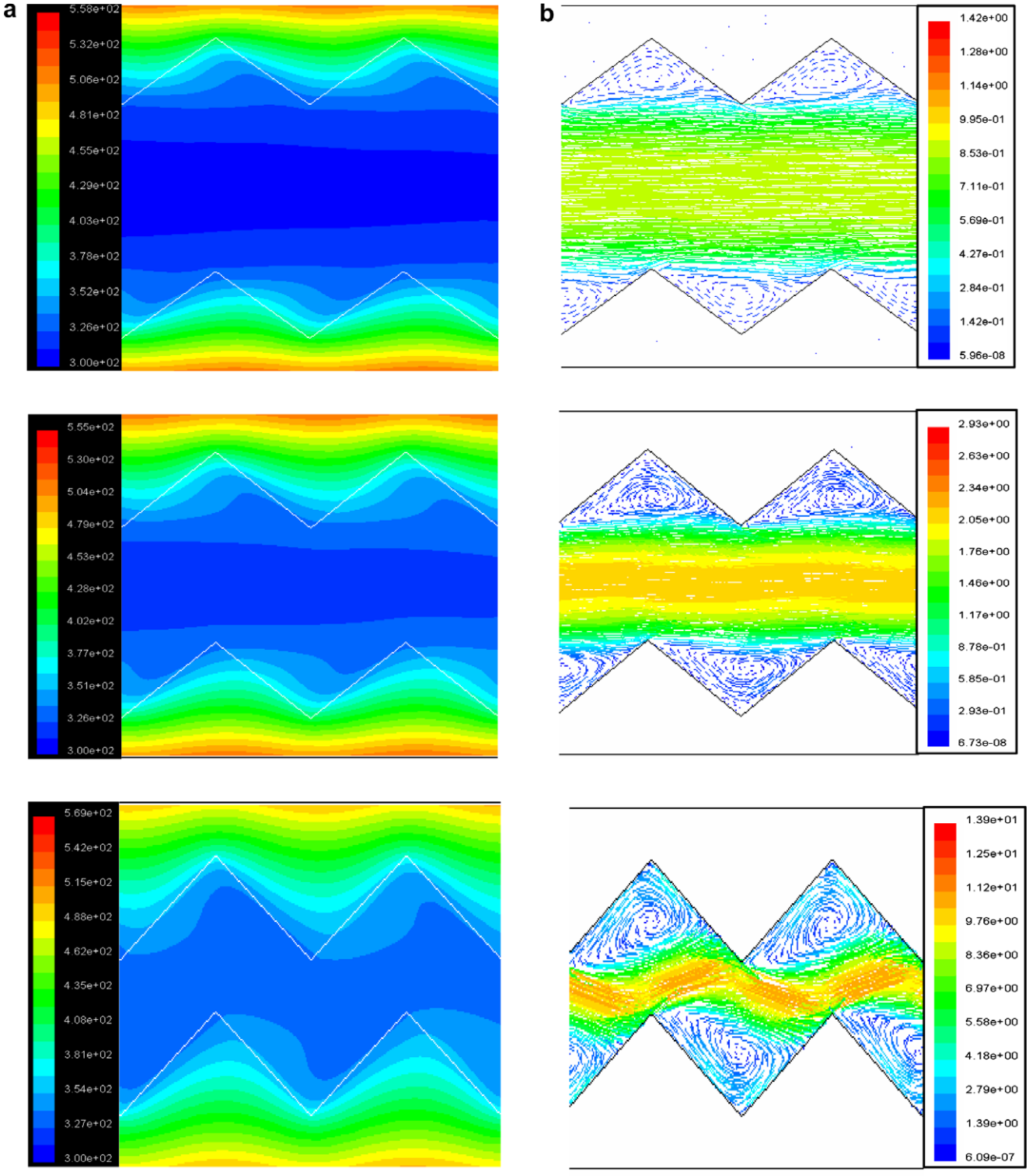

Fig. 11. Variation of (a) temperature contour, (b) velocity vector for different channel heights at the same Re (918), wavy angle = 40°, $q = 0.83$ kW/m^2.

distribution, especially in the narrow channel. From Fig. 11a, due to the growth of the swirl flows in the wall troughs as lower channel height, the temperature gradient between the fluid near the wavy wall and the fluid in the core increase. Therefore, the lower channel height gives the heat transfer rates higher than higher channel height. The change flow structure for the fixed air flow rate ($Re = 9138$) with varying severity of the channel height is shown in Fig. 11b. It can be seen from figure that channel height have significant effect on the dynamic behavior of the fluid flow fields. At the channel height of 12.5 mm, the wavy wall has not significant effect on the flow structure in the core. However, as further decreasing in the channel height, the onset and the growth of the swirl flows encompass much of the bulk flow field, especially in the narrow passage. In addition, the turbulent intensity also increases.

6. Conclusion

New experimental data on the heat transfer and pressure drop characteristics in the channel with double *V*-corrugated surfaces are presented. Breaking and destabilizing in the thermal boundary layer are occurred as fluid flowing through the corrugated surfaces. Using corrugated plates is a suitable method to increase the thermal performance and higher compactness. The effects of wavy angle and channel height have significant effect on the temperature distribution and flow development. The predicted results obtained from the model are validated with the measured data. There is reasonable agreement from the comparison between the predicted results and the measured data. It can be found that the corrugated surface has significant effect on the enhancement of heat transfer and pressure drop.

Acknowledgements

The author would like to express his appreciation to the Srinakharinwirot University (SWU) for providing financial support for this study. The author also wishes to acknowledge Mr. Suthirak Srisuworarutn, Mr. Suradej Kaewma, and Mr. Athaporn Ngamnate for their assistance in some of the experimental work.

References

[1] B. Sunden, T. Skoldheden, Heat transfer and pressure drop in a new type of corrugated channels, Int. Commun. Heat Mass Transfer 12 (1985) 559–566.
[2] B. Sunden, T. Skoldheden, Periodic laminar flow and heat transfer in a corrugated two-dimensional channel, Int. Commun. Heat Mass Transfer 16 (1989) 215–225.
[3] T. Brunner, W. Brenig, Coupled channel calculations for the rotational excitation of molecules at corrugated surfaces, Surface Sci. 201 (1988) 321–334.
[4] E.S. Benilov, M.I. Yaremchuk, On water-wave propagation in a long channel with corrugated boundaries, Wave Motion 13 (1991) 115–121.
[5] R.C. Yalamanchili, Flow of non-Newtonian fluids in corrugated channels, Int. J. Non-Linear Mech. 28 (1993) 535–548.
[6] R.C. Yalamanchili, A. Sirivat, K.R. Rajagopal, An experimental investigation of the flow of dilute polymer solutions through corrugated channels, J. Non-Newtonian Fluid Mech. 58 (1995) 243–277.
[7] D. Sawyer, M. Sen, H.C. Chang, Heat transfer enhancement in three dimensional corrugated channel flow, Int. Commun. Heat Mass Transfer 41 (1998) 3559–3573.
[8] T. Nishimura, S. Matsune, Vortices and wall shear stresses in asymmetric and symmetric channels with sinusoidal wavy walls for pulsatile flow at low Reynolds numbers, Int. J. Heat Fluid Flow 19 (1998) 583–593.
[9] D. Bereiziat, R. Devienne, Experimental characterization of Newtonian and non-Newtonian fluid flows in corrugated channels, Int. J. Eng. Sci. 37 (1999) 1461–1479.
[10] M. Gradeck, M. Lebouche, Two-phase gas-liquid flow in horizontal corrugated channels, Int. J. Multiphase Flow 26 (2000) 435–443.
[11] M. Gradeck, B. Hoareau, M. Lebouche, Local analysis of heat transfer inside corrugated channel, Int. J. Heat Mass Transfer 48 (2005) 1909–1915.
[12] G. Fabbri, Heat transfer optimization in corrugated wall channels, Int. J. Heat Mass Transfer 43 (2000) 4299–4310.
[13] G. Fabbri, R. Rossi, Analysis of the heat transfer in the entrance region of optimised corrugated wall channel, Int. Commun. Heat Mass Transfer 32 (2005) 902–912.
[14] M.A. Mehrabian, R. Poulter, Hydrodynamics and thermal characteristics of corrugated channels: computational approach, Appl. Math. Model. 24 (2000) 343–364.
[15] M. Vasudevaiah, K. Balamurugan, Heat transfer of rarefied gases in a corrugated microchannel, Int. J. Therm. Sci. 40 (2001) 454–468.
[16] B. Niceno, E. Nobile, Numerical analysis of fluid flow and heat transfer in periodic wavy channels, Int. J. Heat Fluid Flow 22 (2001) 156–167.
[17] A. Hamza, H. Ali, Y. Hanaoka, Experimental study on laminar flow forced-convection in a channel with upper *V*-corrugated plate heated by radiation, Int. J. Heat Mass Transfer 45 (2002) 2107–2117.
[18] C. Zimmerer, P. Gschwind, G. Gaiser, V. Kottke, Comparison of heat and mass transfer in different heat exchanger geometries with corrugated walls, Exp. Therm. Fluid Sci. 26 (2002) 269–273.
[19] C.C. Wang, C.K. Chen, Forced convection in a wavy-wall channel, Int. J. Heat Mass Transfer 45 (2002) 2587–2595.
[20] H.M. Metwally, R.M. Manglik, Enhanced heat transfer due to curvature-induced lateral vortices in laminar flows in sinusoidal corrugated-plate channels, Int. J. Heat Mass Transfer 47 (2004) 2283–2292.
[21] Y. Islamoglu, C. Parmaksizoglu, The effect of channel height on the enhanced heat transfer characteristics in a corrugated heat exchanger channel, Appl. Therm. Eng. 23 (2003) 979–987.
[22] Y. Islamoglu, A. Kurt, Heat transfer analysis using ANNs with experimental data for air flowing in corrugated channels, Int. J. Heat Mass Transfer 47 (2004) 1361–1365.
[23] Y. Islamoglu, C. Parmaksizoglu, Numerical investigation of convective heat transfer and pressure drop in a corrugated heat exchanger channel, Appl. Therm. Eng. 24 (2004) 141–147.
[24] M.Z. Hassain, A.K.M. Sadrul Islam, Fully develop flow structures and heat transfer in sine-shaped wavy channels, Int. Commun. Heat Mass Transfer 31 (2004) 887–896.
[25] P. Naphon, Laminar convective heat transfer and pressure drop in the corrugated channels, Int. Commun. Heat Mass Transfer 24 (2007) 62–71.
[26] P. Naphon, Heat transfer characteristics and pressure drop in the channel with *V*-corrugated upper and lower plates, Energy Convers. Manage. 48 (2007) 1516–1524.
[27] P.H. Oosthuizen, D. Nayler, An Introduction to Convective Heat Transfer Analysis, Mc-Graw-Hill, 1999.
[28] B.E. Launder, D.B. Spalding, Mathematical Models of Turbulence, Academic Press, 1973.
[29] H.K. Versteeg, W. Malalasekera, Computational fluid dynamics, Longman Group, 1995.
[30] J.P. Van Doormal, G.D. Raithby, Enhancements of the SIMPLEC method for predicting incompressible fluid flows, Numer. Heat Transfer 7 (1984) 147–163.